Oblique electron-beam evaporation of distinctive indium-tin-oxide nanorods for enhanced light extraction from InGaN/GaN light emitting diodes

C. H. Chiu,[1] Peichen Yu,[1,*] C. H. Chang,[1] C. S. Yang,[1] M. H. Hsu,[1] H. C. Kuo, [1,3] and M. A. Tsai[2]

[1] *Department of Photonics and Institute of Electro-Optical Engineering, National Chiao-Tung University, Hsinchu, Taiwan, R.O.C.*

[2] *Department of Electrophysics, National Chiao-Tung University, Hsinchu, Taiwan, R.O.C.*

[3] *hckuo@faculty.nctu.edu.tw*

* *yup@faculty.nctu.edu.tw*

Abstract: This paper presents a novel and mass-producible technique to fabricate indium-tin-oxide (ITO) nanorods which serve as an omnidirectional transparent conductive layer (TCL) for InGaN/GaN light emitting diodes (LEDs). The characteristic nanorods, prepared by oblique electron-beam evaporation in a nitrogen ambient, demonstrate high optical transmittance (T>90%) for the wavelength range of 450nm to 900nm. The light output power of a packaged InGaN/GaN LED with the incorporated nanorod layer is increased by 35.1% at an injection current of 350mA, compared to that of a conventional LED. Calculations based on a finite difference time domain (FDTD) method suggest that the extraction enhancement factor can be further improved by increasing the thickness of the nanorod layer, indicating great potential to enhance the luminous intensity of solid-state lighting devices using ITO nanorod structures.

OCIS codes: (230.3670) Light-emitting diodes; (220.4241) Nanostructure fabrication.

References and links

1. S. Nakamura, and G. Fasol, *The Blue Laser Diode*, (Springer, New York, 1997).
2. J. Han, M. H. Crawford, R. J. Shul, J. J. Figiel, M. Banas, L. Zhang, Y. K. Song, H. Zhou, and A. V. Nurmikko, "AlGaN/GaN quantum well ultraviolet light emitting diodes," Appl. Phys. Lett. **73**(12), 1688 (1998).
3. Y. Narukawa, I. Niki, K. Izuno, M. Yamada, Y. Murazaki, and T. Mukai, "Phosphor-Conversion White Light Emitting Diode Using InGaN Near-Ultraviolet Chip," J. Appl. Phys. **41**(Part 2, No. 4A), L371–L373 (2002).
4. T. Fujii, Y. Gao, R. Sharma, E. L. Hu, S. P. DenBaars, and S. Nakamura, "Increase in the extraction efficiency of GaN-based light-emitting diodes via surface roughening," Appl. Phys. Lett. **84**(6), 855–857 (2004).
5. D. W. Kim, H. Y. Lee, M. C. Yoo, and G. Y. Yeom, "Highly efficient vertical laser-liftoff GaN-based light-emitting diodes formed by optimization of the cathode structure," Appl. Phys. Lett. **86**(5), 052108 (2005).
6. H. W. Huang, C. C. Kao, J. T. Chu, H. C. Kuo, S. C. Wang, and C. C. Yu, "Improvement of InGaN–GaN light-emitting diode performance with a nano-roughened p-GaN surface," IEEE Photon. Technol. Lett. **17**(5), 983–985 (2005).
7. H. W. Huang, J. T. Chu, C. C. Kao, T. H. Hseuh, T. C. Lu, H. C. Kuo, S. C. Wang, and C. C. Yu, "Enhanced light output of an InGaN/GaN light emitting diode with a nano-roughened p-GaN surface," Nanotechnology **16**(9), 1844–1848 (2005).
8. D. Eisert and V. Harle, "Simulations in the development process of GaN based LEDs and laser diodes," in Int. Conf. Numerical Simulation of Semiconductor Optoelectronic Devices, Session 3: Photonic Devices, invited paper (2002).
9. C. C. Kao, H. C. Kuo, H. W. Huang, J. T. Chu, Y. C. Peng, Y. L. Hsieh, C. Y. Luo, S. C. Wang, C. C. Yu, and C. F. Lin, "Light-output enhancement in a nitride-based light-emitting diode with 22 undercut sidewalls," IEEE Photon. Technol. Lett. **17**(1), 19–21 (2005).
10. Y. J. Lee, J. M. Hwang, T. C. Hsu, M. H. Hsieh, M. J. Jou, B. J. Lee, T. C. Lu, H. C. Kuo, and S. C. Wang, "Enhancing the Output Power of GaN-Based LEDs Grown on Wet-Etched Patterned Sapphire Substrates," IEEE Photon. Technol. Lett. **18**(10), 1152–1154 (2006).
11. J. H. Lee, J. T. Oh, Y. C. Kim, and J. H. Lee, "Stress Reduction and Enhanced Extraction Efficiency of GaN-Based LED Grown on Cone-Shape-Patterned Sapphire," IEEE Photon. Technol. Lett. **20**(18), 1563–1565 (2008).

#117012 - $15.00 USD Received 10 Sep 2009; revised 24 Oct 2009; accepted 24 Oct 2009; published 6 Nov 2009

12. C. H. Chiu, H. C. Kuo, C. E. Lee, C. H. Lin, P. C. Cheng, H. W. Huang, T. C. Lu, S. C. Wang, and K. M. Leung, "Fabrication and characteristics of thin-film InGaN–GaN light-emitting diodes with TiO_2/SiO_2 omnidirectional reflectors," Semicond. Sci. Technol. **22**(7), 831–835 (2007).
13. C. H. Chiu, C. E. Lee, C. L. Chao, B. S. Cheng, H. W. Huang, H. C. Kuo, T. C. Lu, S. C. Wang, W. L. Kuo, C. S. Hsiao, and S. Y. Chen, "Enhancement of Light Output Intensity by Integrating ZnO Nanorod Arrays on GaN-Based LLO Vertical LEDs," Elec. Sol. Sta. Lett. **11**(4), H84–H87 (2008).
14. J. Zhong, H. Chen, G. Saraf, Y. Lu, C. K. Choi, J. J. Song, D. M. Mackie, and H. Shen, "Integrated ZnO nanotips on GaN light emitting diodes for enhanced emission efficiency," Appl. Phys. Lett. **90**(20), 203515 (2007).
15. R. H. Horng, S. H. Huang, C. C. Yang, and D. S. Wuu, "Efficiency Improvement of GaN-Based LEDs with ITO Texturing Window Layers Using Natural Lithography," IEEE J. Sel. Top. Quantum Electron. **12**(6), 1196–1201 (2006).
16. S. Takaki, Y. Aoshima, and R. Satoh, "Growth Mechanism of Indium Tin Oxide Whiskers Prepared by Sputtering," J. Appl. Phys. **46**(No. 6A), 3537–3544 (2007).
17. F. Ishida, K. Yoshimura, K. Hoshino, and K. Tadatomo, "Improved light extraction efficiency of GaN-based light emitting diodes by using needle-shape indium tin oxide p-contact," Phys. Status Solidi **5**(6 c), 2083–2085 (2008).
18. J. K. Kim, S. Chhajed, M. F. Schubert, E. F. Schubert, A. J. Fischer, M. H. Crawford, J. Cho, H. Kim, and C. Sone, "Light-Extraction Enhancement of GaInN Light-Emitting Diodes by Graded-Refractive-Index Indium Tin Oxide Anti-Reflection Contact," Adv. Mater. **20**(4), 801–804 (2008).
19. H. Hashimoto, T. Naiki, T. Eto, and K. Fujiwara, "High Temperature Gas Reaction Specimen Chamber for an Electron Microscope," J. Appl. Phys. **7**(8), 946–952 (1968).
20. H. Hashimoto, A. Kumao, T. Eto, and K. Fujiwara, "Drops of oxides on tungsten oxide needles and nuclei of dendritic crystals," J. Cryst. Growth **7**(1), 113–116 (1970).
21. P. Yu, C. H. Chang, C. H. Chiu, C. S. Yang, J. C. Yu, H. C. Kuo, S. H. Hsu, and Y. C. Chang, "Efficiency Enhancement of GaAs Photovoltaics Employing Anti-Reflective Indium-Tin-Oxide Nano-Columns," Adv. Mater. **21**(16), 1618–1621 (2009).
22. FullWAVE, Rsoft Design Group, Inc.
23. C. H. Chiu, P. Yu, H. C. Kuo, C. C. Chen, T. C. Lu, S. C. Wang, S. H. Hsu, Y. J. Cheng, and Y. C. Chang, "Broadband and omnidirectional antireflection employing disordered GaN nanopillars," Opt. Express **16**(12), 8748–8754 (2008).

1. Introduction

III–nitride-based light-emitting diodes (LEDs) from ultraviolet (UV) to blue/green wavelengths have been intensely researched over the past decade [1,2]. Recently, the increasing brightness of GaN-based LEDs has made possible applications in traffic signals, backlights for cell phones and liquid-crystal-display televisions (LCD-TVs) [3]. However, to replace the conventional fluorescent lighting sources with solid-state lighting devices, additional efforts are required to improve the external quantum efficiency, as well as the light extraction efficiency of UV/blue LEDs. Several methods, including surface roughening techniques [4–7], inclined side-wall etching [8,9], patterned sapphire substrates [10,11], and the incorporation of highly reflective omnidirectional reflectors (ODRs) [12], have been shown to effectively improve the light extraction efficiency. Among these methods, surface roughening is one of the most efficient to provide a large enhancement factor for the extraction efficiency due to increased random scattering events that occur at the roughened surfaces. Multiple approaches that involve photoelectrochemical etching, dry etching, H_3PO_4 wet etching, or excimer laser etching have been proposed and demonstrated nearly two-fold enhancement of light output power [4–7]. However, the etching techniques have inherent limitations for conventional LEDs due to the thin p-GaN top layer. First, the etch depth is limited to the thickness of the p-GaN layer, which is ~200 nm. Therefore, the etching process must be precisely controlled to avoid deterioration of electrical properties. Moreover, although other approaches involving the synthesis of ZnO nanorods and the spin-coating of polystyrene nanospheres have been developed for GaN-based LEDs, separate process steps and foreign materials are unavoidable [13–15]. On the other hand, indium-tin-oxide (ITO) has been widely used in GaN-based LEDs as the transparent conductive layer (TCL) to improve current spreading of the p-GaN layer. In this work, we demonstrate a mass-producible, surface-roughening technique: the oblique evaporation of distinctive indium-tin-oxide (ITO) nanorods on GaN-based LEDs in a nitrogen ambient. The characteristic nanorod layer not only serves as the omnidirectional TCL for LEDs, but also shows enhanced optical transmittance (T>90%) for a broad wavelength range of 450 nm to 900 nm. The light output power of a packaged InGaN/GaN LED with the incorporated nanorod layer is increased by 35.1% at an

#117012 - $15.00 USD Received 10 Sep 2009; revised 24 Oct 2009; accepted 24 Oct 2009; published 6 Nov 2009

injection current of 350 mA, compared to that of a conventional LED. Since the deposition technique is compatible with the conventional fabrication process of LEDs, it not only avoids issues with the etching process, but also allows the growth of high-aspect-ratio nanostructures on the LED surface, pushing the realization of highly luminescent solid state lighting devices.

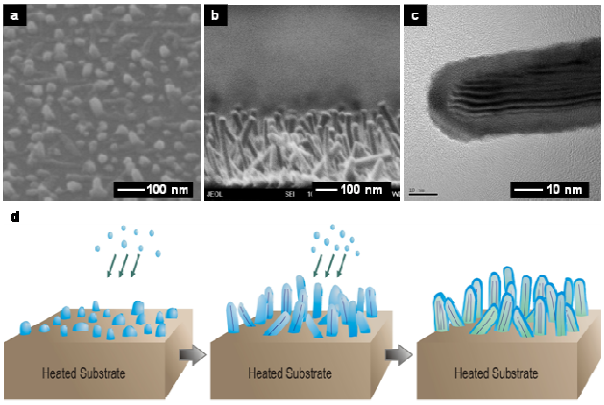

Fig. 1. (a) Scanning electron micrograph of the nucleation cores at the beginning of evaporation, (b) the cross-sectional view of deposited nanorods, (c) the tunneling electron micrograph (TEM) of a nanorod, and (d) schematics for the ITO nanorod growth mechanism.

2. Fabrication and characterization

The characteristic formation of ITO nanorods is assisted by an obliquely incident nitrogen flux using electron-beam evaporation. Although various techniques have been proposed to grow ITO nanostructures [16–18], few have actually resulted in distinctive ITO nanorods with high-aspect ratios. In this work, the nanorods are deposited at a largely inclined angle ~70° with respect to the surface normal of substrates. At the beginning of the evaporation, the chamber pressure is first pumped down to ~10^{-6} torr, followed by the introduction of a nitrogen flow rate at 1 sccm. During the growth, the chamber is stabilized at 260 °C and ~10^{-5} torr with a deposition rate of 0.1nm/sec. Figure 1(a) shows the formation of nucleation cores at the beginning of evaporation. The density could vary from 5x10^{9} cm^{-2} to 2x10^{10} cm^{-2}, depending on the deposition rate and temperature. The deposited nanorods are randomly oriented with heights of 100nm to 300nm and widths of ~40nm, as shown in Fig. 1(b). A high resolution transmission electron microscopic (TEM) image shown in Fig. 1(c) reveals the core-shell structure of an ITO nanorod, where the stripe-like Moiré fringes suggest crystalline material qualities in the center. The energy dispersive X-ray analyses (EDX) also shows that the outer shell possesses a higher tin content than the core region does, indicating the possible occurrence of tin-doped indium segregation during the deposition. Since no apparent catalyst is observed, the nanorod formation presumably involves catalyst-free, vapor-liquid-solid (VLS) phase transitions assisted by the introduced nitrogen [19,20]. The growth mechanism is illustrated in Fig. 1(d). As the indium-oxide and tin-oxide molecules reached the surface of substrates, the random formation of nucleation cores is facilitated by the largely inclined deposition angle ~70° with respect to the surface normal, where the shadow effect may play a role to separate nucleation cores. As opposed to conventional growths of ITO in an oxygen-rich environment, the introduced nitrogen facilitates the segregation of tin-doped indium due to oxygen deficiency during nucleation. As the substrate temperature becomes higher than the melting point of tin-doped indium, the liquid-phase nucleation cores have a large accommodation coefficient to promote the absorption of indium-oxide and tin-oxide vapor via surface diffusion. This process leads to high growth rates in specific directions, resulting in randomly oriented nanorods.

The GaN-based LED structures were grown by metal-organic chemical vapor deposition (MOCVD) on a *c*-plane sapphire substrate. As shown in Fig. 2(a), the epitaxial structures

#117012 - $15.00 USD Received 10 Sep 2009; revised 24 Oct 2009; accepted 24 Oct 2009; published 6 Nov 2009

consisted of a 30-nm-thick low-temperature GaN buffer layer, a 2-μm-thick undoped GaN layer, a 2-μm-thick highly conductive n-type GaN layer, five periods of InGaN/GaN multiple quantum wells, and a 0.2-μm-thick p-type GaN layer. The fabrication of GaN-based LEDs followed a standard four-mask process [6], with a chip size about 1x1 mm^2. After the mesa definition, a 240-nm-thick ITO thin film layer was deposited on p-GaN using an E-gun evaporator, followed by the growth of ITO nanorods at an inclined deposition angle with respect to the surface normal. The evaporation source was composed of tin-oxide (5 wt.%) and indium-oxide (95 wt.%). After the removal of the excess ITO by circumscribing along the edges of the mesa, a metal layer comprising Ni/Au (10nm/120nm) was deposited as the p-type and n-type contact pads. The schematic of a fabricated LED with ITO nanorods is illustrated in Fig. 2 (a), while Fig. 2(b) shows the corresponding photoluminescence spectrum with a dominant emission wavelength located at 460 nm. Finally, the devices were packaged and encapsulated for characterization and lifetime tests. In addition, three samples were also prepared on fused silica substrates for transmission characterizations. The first contains a 240-nm-thick ITO thin film, the second ITO nanorods on a 240-nm-thick ITO thin film, and the third ITO nanorods only.

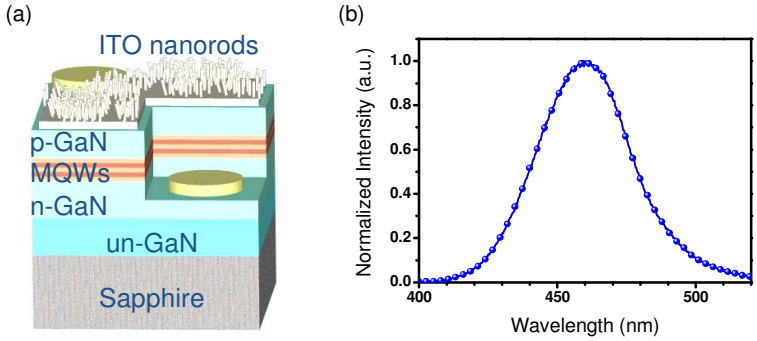

Fig. 2. (a) Schematic diagram of fabricated LEDs with ITO nanorods on the surface and (b) the typical emission spectrum with normalized intensity.

3. Results and discussion

Transmittance spectroscopy was performed using an ellipsometer with a xenon lamp and a monochromator for wavelengths between 350nm and 900 nm. The measured transmittance from different samples was normalized to that of a fused silica substrate. As shown in Fig. 3, the sample with the ITO thin-film only has a relatively high transmittance for 450nm and 720nm wavelengths due to Fabry-Perot resonance. By adding a uniform layer of ITO nanorods on the ITO-coated fused silica, we observed that the transmittance is significantly improved over the entire wavelength range from 350nm to 900nm. For the sample with only ITO nanorods grown on the fused silica substrate, the transmittance for the entire wavelength range is much higher than those of the other two samples. Therefore, we conclude that the ITO nanorods contribute to the enhanced optical transmission by reducing the reflection at the ITO/air interface, thus improving the light extraction of LEDs. It is worth noting that such nanostructures are also very suitable for photovoltaic devices due to the broadband transmission properties [21].

#117012 - $15.00 USD Received 10 Sep 2009; revised 24 Oct 2009; accepted 24 Oct 2009; published 6 Nov 2009

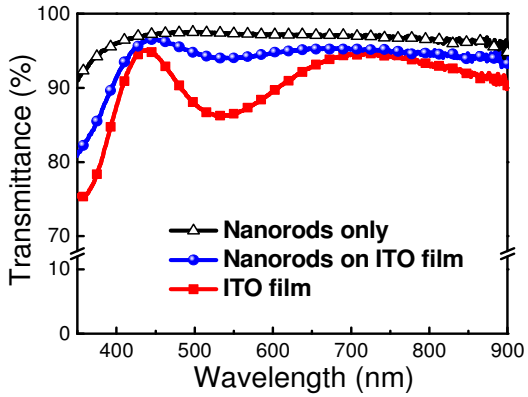

Fig. 3. The normalized transmittance for three samples containing a 240-nm-thick ITO thin film, ITO nanorods grown on the 240-nm-thick ITO thin film, and ITO nanorods only, prepared on fused silica substrates for the wavelength range of 350 to 900 nm.

The current-voltage (I-V) and electroluminescence (EL) characteristics of packaged LEDs with and without ITO nanorods are plotted in Fig. 4. As shown in that figure, the forward voltages of LEDs are 4.08V and 3.99 V at a driving current of 350 mA for devices with and without ITO nanorods, respectively. This nearly identical forward voltage implies that the nanorod deposition does not deteriorate the electrical properties. In addition, the light output power of the LED with ITO nanorods shows ~35.1% enhancement, compared to that of a conventional LED. As discussed previously, the enhanced output power results from the improved transmittance at the roughened surface. The radiation profiles of both devices are also examined at a driving current of 20 mA, as shown in the inset of Fig. 4. The emission pattern from the device with nanorods shows omnidirectional enhancement in the overall integrated intensity. Figure 5 shows the spatial intensity distribution of both devices at an injection current of 200 mA, where 5(a) and 5(b) are images for LEDs with and without the ITO nanorods, respectively. Also, the dark curl structures are pattern electrodes to achieve current spreading for large-area devices. As seen in Fig. 5(a), the light-extraction of the LED with ITO nanorods is evenly enhanced in the spatial domain without deteriorating the current spreading, assuring the practical application of the nanorod deposition technique.

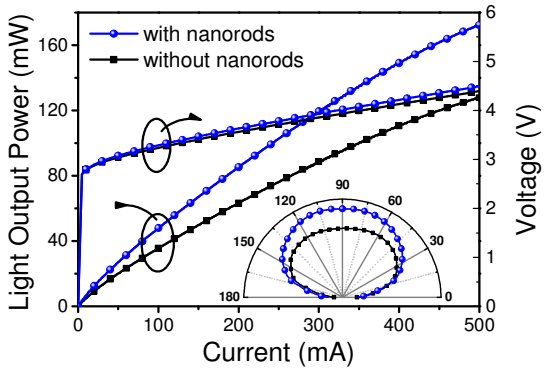

Fig. 4. The current-voltage (I-V) and electroluminescence (EL) characteristics of packaged LEDs with and without ITO nanorods. The inset shows the far-field radiation profile of both devices.

#117012 - $15.00 USD Received 10 Sep 2009; revised 24 Oct 2009; accepted 24 Oct 2009; published 6 Nov 2009

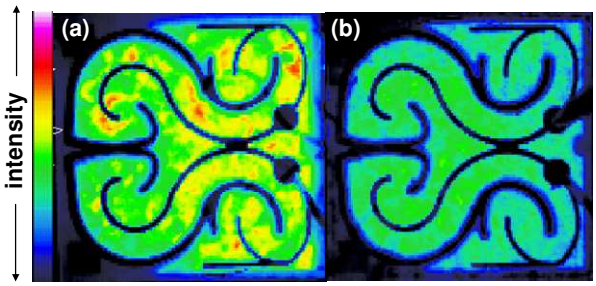

Fig. 5. The spatial intensity distribution of LEDs (a) with and (b) without ITO nanorods at an injected current of 200 mA.

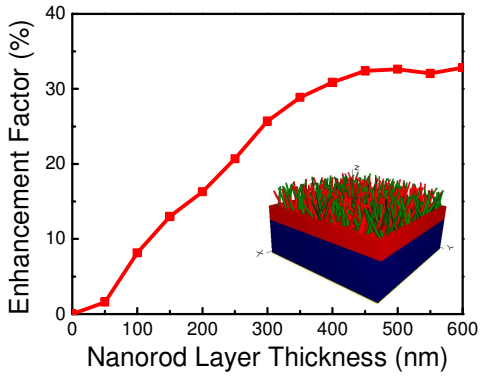

Fig. 6. The calculated enhancement factor versus the thickness of the ITO nanorod layer using a three-dimension finite difference time domain (3D-FDTD) method. The inset shows the modeled index profile.

We further investigate the dependence of light extraction efficiency on the thickness of the ITO nanorod layer using a three-dimensional finite-difference time-domain (3D-FDTD) method [22]. As shown in the inset of Fig. 6, the simulated index profile consists of GaN, a 240nm-thick ITO layer, and 21x21 randomly-positioned and randomly-oriented ITO nanorods placed on top [23]. Here, perfect-matched-layer (PML) boundary conditions are enforced. The material dispersion is also taken into account at the dominant 460nm wavelength. Detail structural parameters of the nanorods are extracted from the SEM pictures shown in Fig. 1(a) and 1(b), and summarized in Table 1. As referred to in Fig. 2(a), the excitation source is located at 2μm below the GaN/air interface and chosen to be spatially incoherent with an excitation area of 2x2 μm^2. The detector that collects the light output is kept at a distance of 1 μm from the ITO nanorod layer. The calculation results are plotted in Fig. 6, where the enhancement factor is defined as the ratio of the change in the extracted power from the nanorod layer divided by the power detected from the ITO layer without nanorods. As shown in Fig. 6, the enhancement factor monotonically increases with the thickness of the nanorod layer and saturates at a maximum value of ~32.5%, when the height is over 450 nm. The calculations suggest that the randomly oriented nanorods behave as a layer with a gradient index profile, instead of a layer with an effective refractive index. The latter often results in an oscillatory dependence of the extracted power on the layer thickness due to the Fabry-Perrot effect. The device behavior, as the nanorod layer thickness increases, implies a gradually changing gradient of the refractive index profile, which is critical to the enhancement of extraction efficiency. As the thickness reaches a certain value, 450nm in this case, the gradient-index profile is no longer the dominant factor to further increase extracted power. Therefore, the enhancement factor saturates. However, we have to note that the calculated enhancement factor is smaller than the measured value of 35.1% for a packaged device at the 350nm thickness, since the measured enhancement factor is generally larger for a non-

#117012 - $15.00 USD Received 10 Sep 2009; revised 24 Oct 2009; accepted 24 Oct 2009; published 6 Nov 2009

packaged device(>40%). The discrepancy may be attributed to the defined nanorod profile not being fully representative to the grown structure. We are currently conducting experiments to verify the dependence of the enhancement factor on the nanorod layer thickness.

Table 1. Defined structural parameters for 21x21 randomly oriented and positioned nanorods.

Structural parameters of nanorods	
Density	1.0×10^{10} cm^{-2}
Base diameter	50 nm
Top diameter	30 nm
Average height (L)	0-600 nm
Height variation	± 0.25L
Position variation	± 25nm

Finally, a lifetime test was conducted for the LEDs with and without ITO nanorods driven by 350 mA injection current at room temperature. As shown in Fig. 7, the normalized EL intensity is shown as a function of the aging time. After a 1000 hr life test, the LED with the nanorod layer shows a comparable decaying trend as the one without nanorods. The normalized output power for both devices was decreased by merely 7–11%. The test result further confirms that the deposited nanorod layer could effectively improve device performance without any auxiliary effects, making it very suitable for commercial devices.

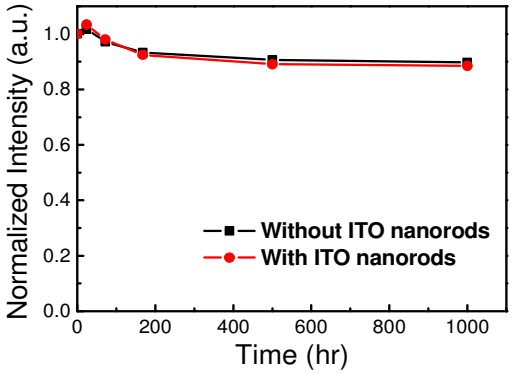

Fig. 7. Lifetime test of LEDs with and without ITO nanorods over 1000 hours under an injection current of 350 mA.

4. Conclusion

In summary, a distinctive ITO nanorod layer was successfully demonstrated using oblique electron-beam evaporation in a nitrogen-rich environment, where the formation involves a catalyst-free VLS mechanism. The characteristic ITO nanorods exhibited high transmittance over a broad wavelength range. LEDs with the nanorod layer show an enhanced light output power of 35.1% at an injection current of 350 mA, compared to conventional LEDs. Calculations based on a 3D-FDTD method suggest that the ITO nanorod layer improves the light extraction efficiency by behaving as a gradient-index layer, where the enhancement factor increases with the thickness of the nanorod layer up to 32.5%.

Acknowledgements

This work was supported by the National Science Council in Taiwan under grant number, NSC98-2120-M-006-003, NSC-95-2622-E009-013-CC3, and NSC 96-2221-E-009-092-MY3

#117012 - $15.00 USD Received 10 Sep 2009; revised 24 Oct 2009; accepted 24 Oct 2009; published 6 Nov 2009